# Selective exhaust gas recirculation in combined cycle gas turbine power plants with post-combustion $CO_2$ capture

**Citation for published version:**
Herraiz, L, Fernández, ES, Palfi, E & Lucquiaud, M 2018, 'Selective exhaust gas recirculation in combined cycle gas turbine power plants with post-combustion $CO_2$ capture', *International Journal of Greenhouse Gas Control*, vol. 71, pp. 303-321. https://doi.org/10.1016/j.ijggc.2018.01.017

**Digital Object Identifier (DOI):**
10.1016/j.ijggc.2018.01.017

**Link:**
Link to publication record in Heriot-Watt Research Portal

**Document Version:**
Peer reviewed version

**Published In:**
International Journal of Greenhouse Gas Control

# Selective exhaust gas recirculation in combined cycle gas turbine power plants with post-combustion $CO_2$ capture

Laura Herraiz[a,]*, Eva Sánchez Fernández[b], Erika Palfi[a], Mathieu Lucquiaud[a]

[a] *The University of Edinburgh, School of Engineering, The Kings Buildings, Edinburgh EH9 3JL, United Kingdom*

[b] *Heriot-Watt University, Institute of Petroleum Engineering, Edinburgh EH14 4AS, United Kingdom*

**Appendix A. Design Basis and description of the CCGT power plant and the PCC system for the reference configuration.**

***A.1.- Ambient conditions***

Table A.1.- Ambient conditions

| | | |
|---|---|---|
| Pressure (ISO) | kPa | 101.325 |
| Temperature (ISO) | ºC | 15 |
| Relative humidity, $\phi$ | % | 60 |
| *Composition, dry molar fraction (%)* | | |
| $N_2$ | %vol | 78.08 |
| $CO_2$ | %vol | 0.03 |
| $H_2O$ | %vol | 0.00 |
| Ar | %vol | 0.94 |
| $O_2$ | %vol | 20.95 |
| Molar Mass | g/mol | 28.86 |

***A.2.- Natural gas***

Table A.2.- Natural gas supply specifications

| | | |
|---|---|---|
| Fuel type | Natural Gas | |
| Supply temperature | ºC | 10 |
| Supply pressure | MPa | 7 |
| *Composition, molar fraction (%)* | | |
| $CH_4$ | %vol | 89 |
| $C_2H_6$ | %vol | 7 |
| $C_3H_8$ | %vol | 1 |
| $C_4H_{10}$ | %vol | 0.11 |
| $N_2$ | %vol | 0.89 |
| $CO_2$ | %vol | 2 |
| S | ppm | <5 |
| Molar mass | g/mol | 17.84 |
| $CO_2$ emissions | g/kWh LHV | 208.00 |
| *Heating values* | | |
| Low heat value (LHV) @ 25 ºC | MJ/kg | 46.94 |
| High heat value (HHV) @ 25 ºC | MJ/kg | 51.58 |

***A.3.- Design and operating parameters for the CCGT plant in the reference configuration.***

The reference plant is an air-based combustion CCGT with a 2-on-1 configuration: two GE Class F (GE9371B) gas turbines with the flue gas exiting into two HRSGs, which jointly supply steam to a subcritical triple pressure steam cycle. The reference power plant is designed according to the configuration of a report commissioned by the International Energy Agency Greenhouse Gas R&D programme (IEA 2012). The net power output and the thermal efficiency of the CCGT plant equipped with PCC is presented in Table A.3. Design and operating parameters of the gas turbine engine are presented in Table A.4 and have been obtained from General Electric technical specifications (General Electric Power Generation 2016) and data from journal publications using the same class of gas turbine engine (Sánchez et al. 2010, Jordal et al. 2012, Jonshagen et al. 2011, Chacartegui et al. 2012). Design and operating parameters of the HRSG are presented in Table A.5 and technical details of the steam turbines are presented in Table A.6.

Table A.3.- Power output and thermal efficiency for the air-based combustion CCGT in the reference configuration

| **Combined Cycle Gas Turbine plant** | | |
|---|---|---|
| Gas turbine net power per GT-HRSG train | MWe | 285.8 |
| Gas turbines net power | MWe | 571.6 |
| Open cycle thermal efficiency | % LHV | 38.18 |
| Steam turbine power | MWe | 256.0 |
| Fuel heat input per GT-HRSG train | MWth | 748.0 |
| CCGT gross power | MWe | 827.6 |
| CCGT gross thermal efficiency | % LHV | 55.50 |
| **CCGT net power output** | **MWe** | **777.44** |
| **CCGT net thermal efficiency** | **%** | **51.94** |

Table A.4.- Gas turbine engine design parameters per GT-HRSG train in the reference configuration

| **Gas turbine** | | | |
|---|---|---|---|
| **Model** | | | **GE 9371FB** |
| Air mass flow rate | | kg/s | 641.81 |
| Fuel mass flow rate | | kg/s | 16.10 |
| **Compressor** | | | |
| No. stages | | -- | 18 |
| Inlet pressure drop | | kPa | 1 |
| Pressure ratio (PR) | | -- | 18.1 |
| Compressor isentropic efficiency | | % | 79.5% |
| **Combustor** | | | |
| Pressure drop | | % | 5 |
| Combustor efficiency | | % | 99.8% |
| P fuel in | | bar | 27.20 |
| T fuel in | | ºC | 117 |
| **Turbine** | | | |
| No. stages | | -- | 4 |
| Turbine inlet temperature (TIT) | | ºC | 1371 |
| Turbine inlet temperature (TIT) | | K | 1644 |
| Turbine back pressure | | bar | 1.039 |
| Turbine isentropic efficiency | | % | 90.5% |
| **Exhaust flue gas (EFG)** | | | |
| Pressure | | kPa | 103.9 |
| Temperature | | ºC | 643.29 |
| Exhaust flue gas flow rate | | kg/s | 657.92 |
| Composition: | | | |
| | $CO_2$ | %vol | 4.21% |
| | $H_2O$ | %vol | 8.82% |
| | $N_2$ | %vol | 74.21% |
| | $O_2$ | %vol | 11.87% |
| | Ar | %vol | 0.89% |
| Molar mass | | g/mol | 28.38 |
| **Gas turbine performance** | | | |
| Mechanical efficiency compressor | | % | 99.6 |
| Net Power | | MW | 285.76 |
| Net Thermal efficiency | | % | 38.18 |
| Net Heat Rate | | kJ/kWh | 9428.07 |

Table A.5.- Heat recovery steam generator design parameters per GT-HRSG train for the reference configuration

| **Heat recovery steam generator** | | |
|---|---|---|
| **Flue gas** | | |
| Flue gas mass flow rate | kg/s | 657.92 |
| Gas Inlet temperature | ºC | 643.29 |
| Gas Outlet temperature | ºC | 117.87 |
| Feed water temperature | ºC | 32.28 |
| Gas inlet pressure | bar | 1.039 |
| Gas outlet pressure | bar | 1.013 |
| HRSG efficiency | % | 99.7 |
| **Pressure levels** | | |
| HP drum pressure | bar | 173 |
| IP drum pressure | bar | 43 |
| LP drum pressure | bar | 4 |
| **Temperature differences** | | |
| ΔT approach main steam | ºC | 42.5 |
| ΔT approach hot reheated steam | ºC | 34 |
| ΔT pinch gas boiling - liquid in evaporator | ºC | 10 |
| ΔT subcooling economiser | ºC | 3 |
| **Pressure losses** | | |
| ΔP gas side | kPa | 2.6 |
| ΔP HP SH | % | 3.5 |
| ΔP HP ECO | % | 2.6 |
| ΔP IP RH | % | 3 |
| ΔP IP SH | % | 2 |
| ΔP IP ECO | % | 3 |
| ΔP LP SH | % | 2 |
| ΔP LP ECO | % | 1.3 |
| ΔP system - LIVE STEAM | | |
| ΔP system - COLD RH | % | 7 |
| ΔP system- HOT RH | % | 9 |
| ΔP system - LP STEAM | % | 9 |
| **Temperature losses** | | |
| From superheater / reheater to turbine (approximately 0.5 K) | kJ/kg | 1 |
| **Condenser** | | |
| Presure condenser | kPa | 4.814 |
| Saturation temperature | ºC | 32.20 |
| Temperature pinch | ºC | 3.2 |
| Feed water temperature (after feed water pump) | ºC | 32.2 |
| Cooling water supply (CWS) temperature | ºC | 18 |
| Cooling water return (CWR) temperature | ºC | 29 |
| Condenser duty | MW | 224.3 |
| Power to thermal duty (Electric consumption for heat rejection of rejected thermal power) | % | 0.8 |
| **Fuel heater** | | |
| Fuel Inlet Temperature | ºC | 9.00 |
| Fuel Outlet Temperature | ºC | 117.00 |
| IP water inlet temperature | ºC | 252.85 |
| Temperature pinch | ºC | 26.98 |
| **Efficiency calculations** | | |
| Pump efficiency | % | 70 |
| Generator efficiency | % | 98.5 |

Table A.6.- Steam turbines design and operating parameters for the two GT-HRSG trains for the reference configuration.

| **Steam turbines** | | |
|---|---|---|
| ***HP STEAM TURBINE*** | | |
| Live steam molar flow | mol/s | 9587 |
| Live steam mass flow | tn/h | 621 |
| P in | bar | 170 |
| T in | ºC | 600 |
| P out | bar | 45.2 |
| T out | ºC | 394 |
| Isentropic efficiency | % | 88.1% |
| ***IP STEAM TURBINE*** | | |
| Hot reheated molar flow | mol/s | 10445 |
| Hot reheated mass flow | tn/h | 677 |
| P in | bar | 40 |
| T in | ºC | 600 |
| P out | bar | 3.75 |
| T out | ºC | 266.8 |
| Isentropic efficiency | % | 92.4% |
| ***LP STEAM TURBINE*** | | |
| Turbine exhaust molar flow | mol/s | 5595 |
| Turbine exhaust mass flow | tn/h | 363 |
| P in | bar | 3.75 |
| T in | ºC | 266.93 |
| P out | bar | 0.0481 |
| Exhaust steam quality | % | 91.9% |
| Isentropic efficiency | % | 88.0% |

***A.4.- Design and operating parameters for the $CO_2$ capture plant in the reference configuration***

The carbon capture process is modelled in Aspen Plus V7.0 commercial software (Aspen Tech). The process flow diagram of the conventional MEA based chemical absorption process, as set up in Aspen Plus, is illustrated in Figure A.1. Design parameters are presented in Table A.7 and results from the model are presented in Table A.8. The electrolyte non-random two-liquid (E-RNTL) thermodynamic package is selected to describe the $CO_2$-$H_2O$-MEA chemistry in the liquid phase, and the Peng-Robinson equation of state for the gas phase.

The absorption process consists of three unit operations: direct contact cooler, absorber and water wash section. The absorber is simulated with a rate-based model which includes reaction kinetics, thermodynamic equilibrium, mass transfer and heat transfer phenomena. The reactions between $CO_2$ and MEA are very fast and take place in the liquid phase with no reaction in the gas phase (Razi et al. 2013). Mass and heat transfer rates between the contacting phase are therefore based on the combined diffusion-reaction process in the liquid phase, while phase equilibrium exists at the interface. For the gas phase only diffusional resistance is taken into account. Effective interfacial area and liquid side mass transfer coefficients are determined using Bravo-Rocha-Fair correlations (Bravo et al 1982, Bravo et al 1985) which are valid for structured packing Sulzer Mellapak 250Y, and heat transfer coefficients are predicted by the Chilton and Colburn analogy. The bulk properties are evaluated at the outlet conditions for the liquid phase (well mixed flow model) and at average conditions for the vapor phase (plug flow model). The kinetic model of the $CO_2$-MEA-$H_2O$ system considered in Razi's work, where results from the absorber model were in good agreement with experiment data sets from the Esbjerg CESAR ($CO_2$ Enhanced Separation and Recovery) pilot plant, for $CO_2$ capture with aqueous MEA solution at 30 wt% from a flue gas slip of a 400 MWe pulverized coal-fired power plant (Razi et al. 2013; Sanchez Fernandez et al. 2014). The modelling results for the reference case, a CCGT plant with PCC, are compared to data from a test campaign with 30 wt% MEA at the $CO_2$ Technology Centre, in Mongstad, Norway (Hamborg et al. 2014).

The lean-rich solvent heat exchanger is designed on the basis of a fixed overall heat transfer coefficient and a temperature approach of 8 ºC (cold out – hot in approach).

The stripper is simulated with an equilibrium model. Due to the high operating temperature, the kinetic of the reactions is fast and the process is thermodynamically controlled. Moreover, a high temperature enhances the mass transfer and mass transfer resistance is neither the limiting step. The stripper is designed to achieve a fixed molar $CO_2$ recovery ratio and the number of equilibrium stages is consequently defined. The $CO_2$ recovery ratio is set to control the lean solvent $CO_2$ loading at which the stripper column operates and this value is selected to bring the specific heat consumption to a minimum.

Table A.7.- Design parameters of the PCC system for the reference configuration

| | | |
|---|---|---|
| ***Flue gas conditioning system*** | | |
| Booster fan pressure ratio | bar | 0.1 |
| Booster fan isentropic efficiency | % | 85 |
| Booster fan mechanical efficiency | % | 95 |
| Direct contact cooler flue gas outlet temperature | ºC | 45 |
| Direct contact cooler + rotary heat exchanger pressure drop | bar | 0.05 |
| ***Absorber*** | | |
| Solvent | | MEA |
| Concentration | %wt. | 30 |
| Lean solvent temperature | ºC | 40 |
| Flue gas inlet temperature | ºC | 45 |
| Flue gas temperature water wash outlet | ºC | 45 |
| Absorber column pressure | bar | 1.1 |
| Flooding factor | % | 80 |
| Packing | | Mellapak 250 Y |
| Absorber column pressure drop | mbar | 50 |
| ***Lean/rich heat exchanger*** | | |
| Lean/rich heat exchanger DT min | ºC | 8 |
| Lean/rich stream heat exchanger pressure drop | kPa | 20 |
| Rich pump outlet pressure | bar | |
| ***Stripper*** | | |
| Stripper column pressure drop | mbar | 300 |
| Stripper column number of stages | -- | 8 |
| Flooding factor | % | 80 |
| ***Reboiler*** | | |
| Reboiler pressure / saturated | bar | 3 |
| Saturated steam inlet temperature | ºC | 133 |
| Lean solvent outlet temperature | ºC | 120 |
| Pinch temperature | ºC | 13 |
| ***Lean/ Rich solvent pumps*** | | |
| Pumps hydraulic efficiency | % | 75 |
| Pumps driver efficiency | % | 95 |

Table A.8.- Operating parameters of the PCC plant for the reference configuration per GT-HRSG train

| CASE | Air-based combustion (reference case) | |
|---|---|---|
| Overall $CO_2$ capture level | % | 90 |
| **Absorber** | | |
| *Flue gas BOTTOM* | | |
| Mass flow rate | kg/s | 658 |
| $CO_2$ conc. | %vol | 4.21 |
| *Flue gas TOP* | | |
| $CO_2$ conc. | %vol | 0.43 |
| Absorber efficiency | % | 90 |
| Rich solvent loading | $mol_{CO2}/mol_{MEA}$ | 0.26 |
| Lean solvent loading | $mol_{CO2}/mol_{MEA}$ | 0.458 |
| Lean solvent molar flow rate | mol/s | 886 |
| *Absorber dimensions* | | |
| No. Absorbers | -- | 2 |
| Diameter | m | 12 |
| Packing height | m | 19 |
| Total packing volume per GT+HRSG train | $m^3$ | 4190 |
| **Stripper** | | |
| Stripper pressure | bar | 1.84 |
| Steam specific consumption | kg/kg $CO_2$ | 1.71 |
| Specific reboiler duty | MJ/kg $CO_2$ | 3.746 |
| $CO_2$ to pipeline | kg/s | 76.5 |
| **$CO_2$ compression train** | | |
| $CO_2$ final pressure | bar | 110 |
| Specific compression work | kJ/kg $CO_2$ | 334 |

### *A.5.- Design and operating parameters for the $CO_2$ compression train in the reference configuration*

The $CO_2$-rich gas stream leaves the condenser of the stripper column at 40 ºC and 2 bar, with a $CO_2$ purity of 95 vol% and needs to be conditioned prior to transport and storage/utilization. The $CO_2$-rich stream is compressed up to around the critical pressure (73.8 bar) in the compression train, which consists of three stages with intercooling and water separation between stages. Liquid phase $CO_2$ at 73 bar and 28 ºC is pumped up to 110 bar for transfer and storage in supercritical/dense phase. The operating parameters are based on the Common Framework Definition Document published by the European Benchmarking Task Force (EBTF 2011). The process flow diagram of the compressor train is illustrated in Figure A.2. Design and operating parameters are presented in Table A.9.

Table A.9.- Design parameters and operating variables of the $CO_2$ compression train for the reference configuration.

| *CO2 compression plant* |
|---|

| | | |
|---|---|---|
| Final delivery pressure | bar | 110 |
| $CO_2$ purity | % | 99.8 |
| Compression stages pressure ratios | -- | 4.3 / 4.3 / 3.7 |
| Compressor isentropic efficiency | % | 85 |
| Compressor mechanical efficiency | % | 95 |
| Intercooler stages | -- | 3 |
| Intercoolers outlet temperature | ºC | 28 |
| Pump efficiency | % | 75 |
| Pump delivery pressure | bar | 110 |

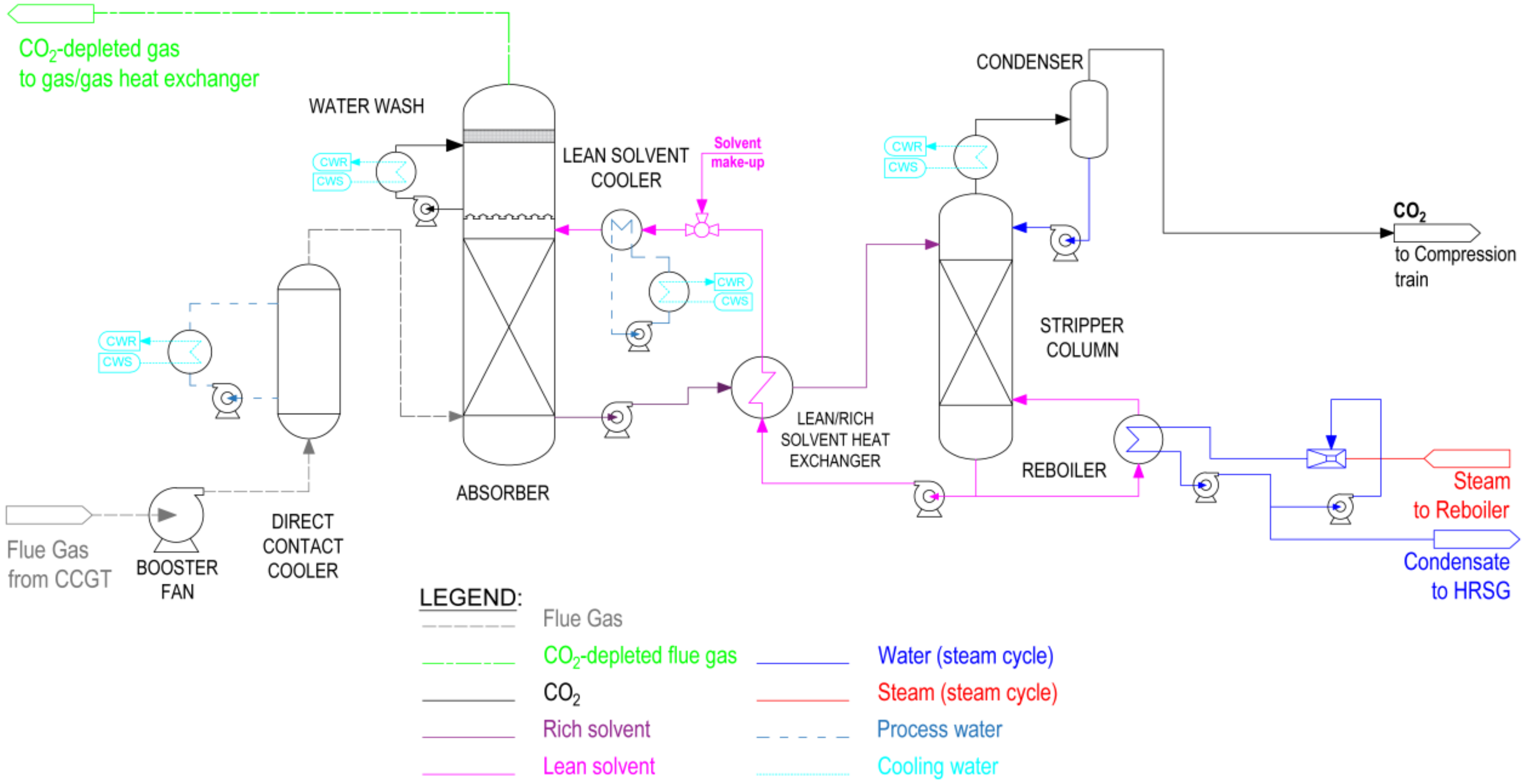


Figure A.1.- Process flow diagram of the post-combustion $CO_2$ capture system with amine-based chemical absorption technology.

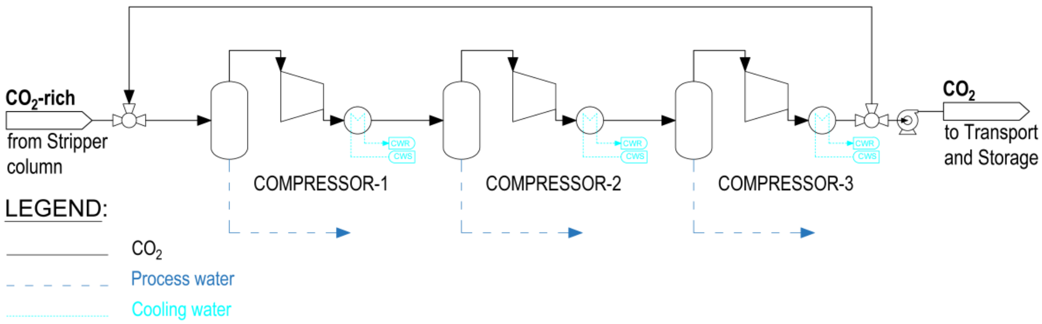


Figure A.2.- Process flow diagram of the $CO_2$ compression train.

## Appendix B. Sizing and optimisation of the PCC system with SEGR

The procedure followed to size and optimise the PCC system is described here and illustrated in Figures B.1, for SEGR in parallel operating at 97% PCC efficiency, and in Figure B.2, for SEGR in series operating at 31% PCC efficiency.

*Absorber sizing*

Operating and design parameters in the $CO_2$ capture system are evaluated following the procedure described by Freguia and Rochelle (Freguia and Rochelle 2003) to achieve the $CO_2$ capture efficiency in the PCC process that is required in each configuration for a 90% overall $CO_2$ capture level. The absorber diameter is determined for a flue gas velocity that corresponds to 80% of the velocity at the flood-point (Oexmann, Hensel and Kather, 2008). The absorber packing height is then increased for a constant diameter. A larger packing volume results in a larger contact surface area and a longer residence time, which enhances the $CO_2$ absorption rate and, thus, the $CO_2$ loading of the solvent at the bottom of the absorber (rich solvent). For a constant lean solvent $CO_2$ loading, it results in an increased solvent capacity and, thus, less amount of solvent is required to achieve certain $CO_2$ absorption efficiency. The absorber packing height is augmented up to a value at which a further increase results in a marginal gain in the rich solvent $CO_2$ loading (< 0.2% of the previous value) and in a marginal reduction of the reboiler duty. The absorber packing height is optimised for each one of the considered configurations.

*Reboiler duty optimisation*

The thermal energy supplied in the reboiler by condensing steam is used in the stripper column to provide: the sensible heat required to heat up the solvent to the reboiler temperature, the heat of desorption of $CO_2$ required to reverse the chemical reactions between the amine and the $CO_2$ and release $CO_2$ into the vapor phase, and the latent heat for vaporisation of water to produce the stripping steam. The steam is condensed in the overheat condenser at 40 ºC. The condensed water returns to the stripper as reflux and the $CO_2$ rich gas is sent to the compression train.

For conventional MEA solvent, the maximum allowable regeneration temperature is around 120 ºC to prevent from thermal degradation, i.e. polymerisation (Rochelle, 2012). The temperature of the condensing steam in the reboiler exceeds the solvent temperature by the pinch temperature assumed in the reboiler design, i.e. 13 ºC (Sanchez Fernandez et al. 2014). Saturated steam at 133 ºC and 3 bar is supplied from the power plant steam cycle.

The optimum lean solvent flow rate entering the absorber which minimises the specific reboiler duty, in MJ/kg $CO_2$, is evaluated for each configuration. The conditions in the stripper are set to achieve the lean solvent $CO_2$ loading resulting in the required $CO_2$ capture efficiency in the absorber to achieve an overall $CO_2$ capture level of 90%. The overall $CO_2$ capture level takes into account the amount of $CO_2$ exiting the boundaries of the plant.

The control strategy to vary the lean solvent $CO_2$ loading can be designed by varying either the temperature or the pressure in the stripper column. A constant temperature of the saturated stream supplied to the reboiler of 120 ºC is assumed here and the total pressure in the stripper column is modified, i.e. with a back pressure valve. The saturated steam flow is evaluated to supply the reboiler duty necessary to achieve the lean solvent $CO_2$ loading.  A smaller total pressure results in a smaller $CO_2$ partial pressure, as the water vapour partial pressure is almost constant at a given temperature. This fact displaces the equilibrium towards a lower $CO_2$ loading of the lean solvent, according to the vapour-liquid equilibrium curve. The larger solvent capacity results in a smaller solvent flow rate to capture 90% of the $CO_2$ generated in the combustion. An increase in the total pressure results in a higher $CO_2$ loading of the lean solvent and, thus, a larger solvent flow rate is necessary.

The effect on the reboiler duty is that the contribution of the sensible heat increases directly proportional to the solvent flow rate and, thus, becomes more significant at a higher lean solvent $CO_2$ loading. Meanwhile, the contribution of the latent heat for steam generation is more relevant at a lower solvent flow rate as more steam needs to be generated to strip off the $CO_2$ and achieve low lean solvent $CO_2$ loadings. There is therefore an optimal value of the lean solvent $CO_2$ loading that results in a minimum specific reboiler duty.

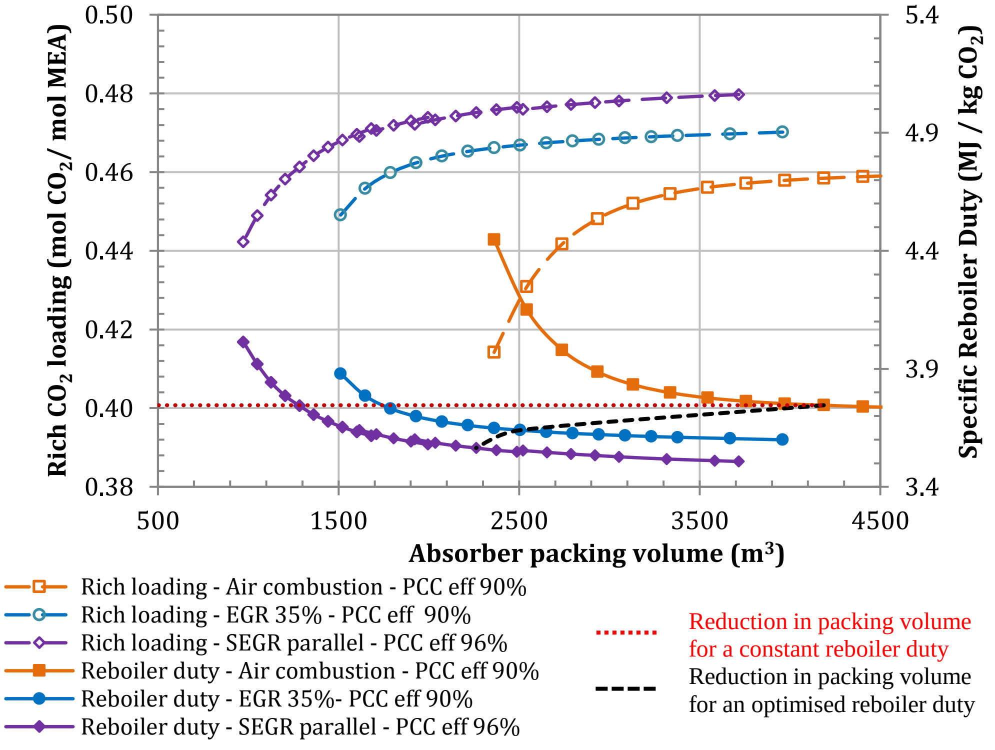


**Figure B.1.-** Sensitivity of the rich solvent $CO_2$ loading and the specific reboiler duty to the packing volume for S-EGR in parallel at 70% recirculation ratio and 96% post-combustion $CO_2$ capture efficiency. Compared to air-based combustion configuration and EGR at 35% recirculation ratio and 90% post-combustion $CO_2$ capture efficiency.

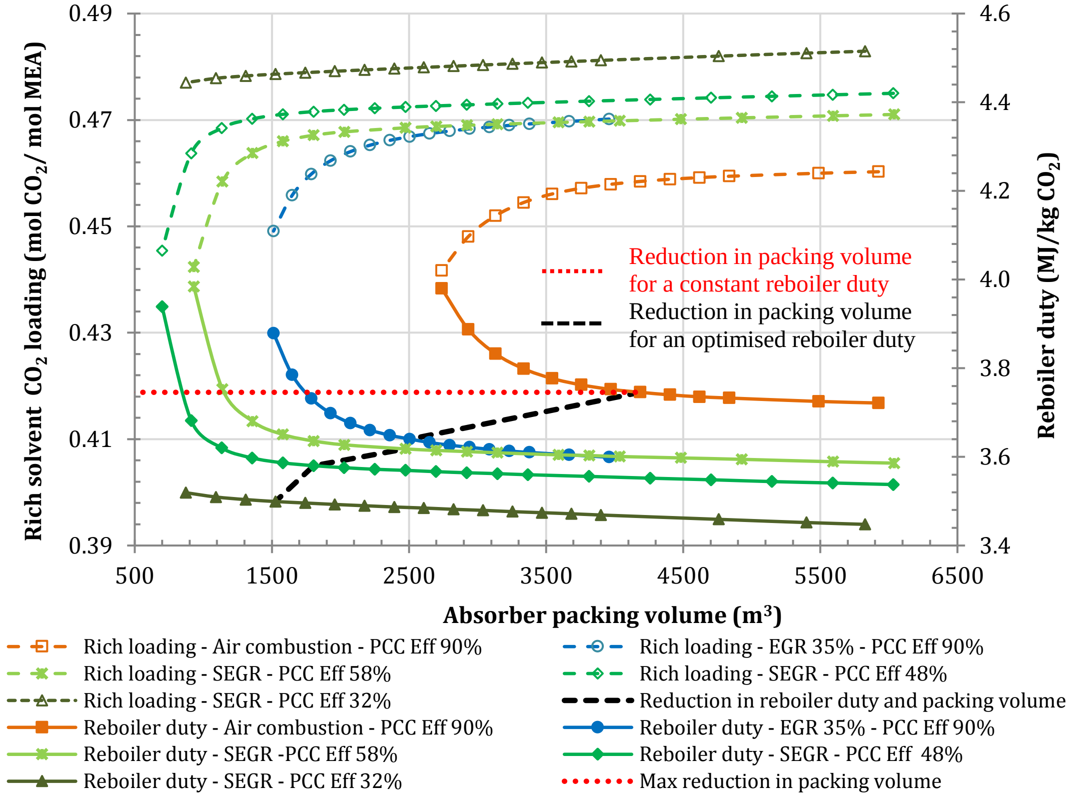


**Figure B.2.-** Sensitivity of the rich solvent $CO_2$ loading and the specific reboiler duty to the packing volume for S-EGR in series for the configurations operating at 32%, 48% and 58% $CO_2$ capture efficiency. Compared to air-based combustion configuration and EGR at 35% recirculation ratio for 90% $CO_2$ capture efficiency.

## Appendix C. Heat transfer and temperature diagram in the HRSGs for a CCGT plant with SEGR and PCC.

The gas and water/steam temperature profile as a function of the heat transfer flow rate is shown in Figure C.1, for SEGR in parallel 97/96, and Figure C.2, for SEGR in series 95/31.

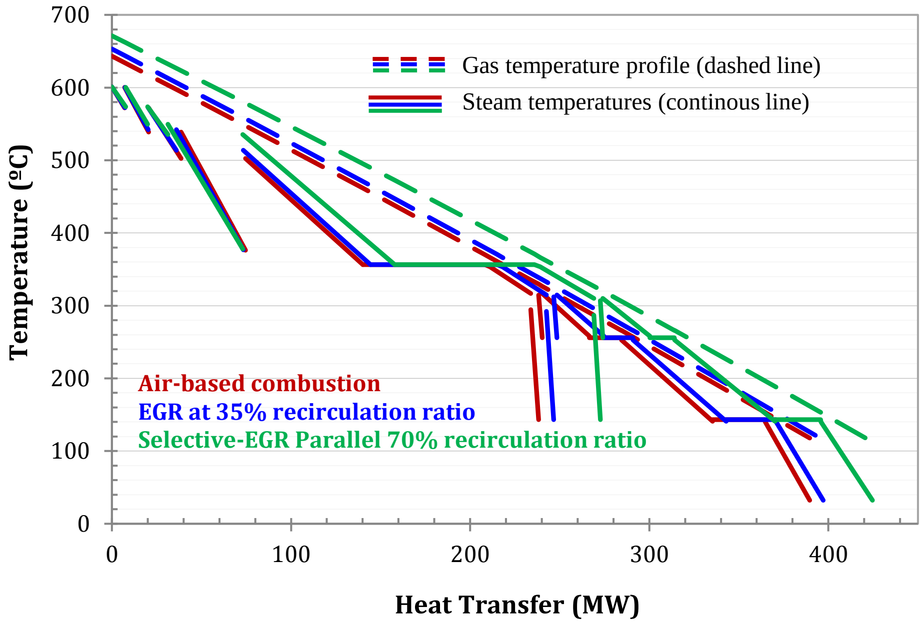


**Figure C.1.-** Heat transfer – temperature diagram for S-EGR configuration in parallel at 70% recirculation ratio, 97% selective $CO_2$ transfer efficiency and 96% post-combustion $CO_2$ capture efficiency, compared to air-based combustion and EGR at 35% recirculation ratio configurations.

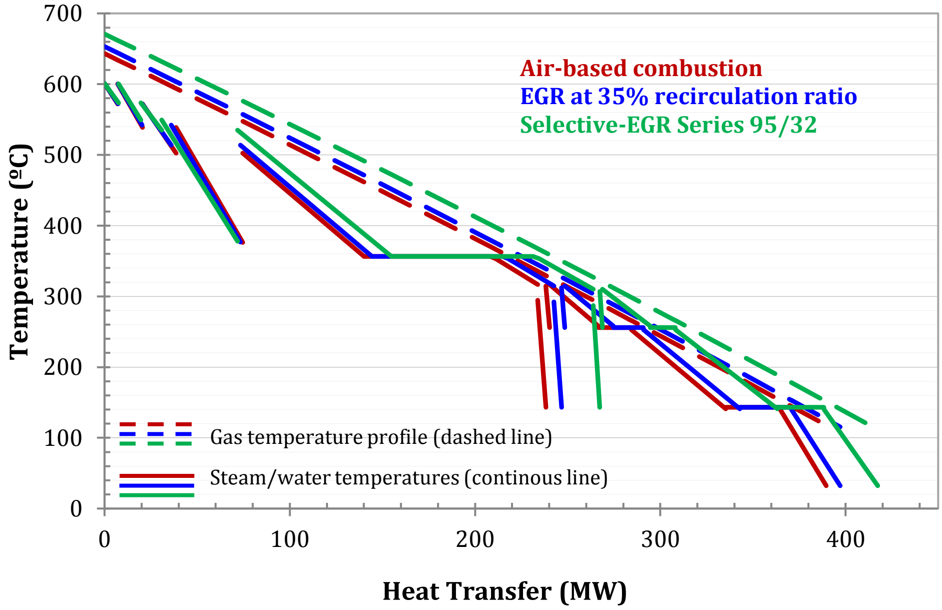


**Figure C.2.-** Heat transfer – temperature diagram for S-EGR in series configuration, with 95% selective $CO_2$ transfer efficiency and 32% post-combustion $CO_2$ capture efficiency, compared to air-based combustion and EGR at 35% recirculation ratio diagrams.